Surface & Coatings Technology 232 (2013) 412–418

Contents lists available at ScienceDirect

Surface & Coatings Technology

journal homepage: www.elsevier.com/locate/surfcoat

Electrochemical corrosion properties of the surface layer produced by supersonic fine-particles bombarding on low-carbon steel

Liuyan Zhang [a], Aibin Ma [a,b,*], Jinghua Jiang [a,b], Dan Song [a], Donghui Yang [a], Jianqing Chen [a]

[a] College of Mechanics and Materials, Hohai University, Nanjing 210098, PR China
[b] Nano-structure Materials Center, School of Materials Science and Engineering, Nanjing University of Science and Technology, Nanjing 210094, PR China

ARTICLE INFO

Article history:
Received 19 March 2013
Accepted in revised form 28 May 2013
Available online 5 June 2013

Keywords:
Supersonic fine-particles bombarding
Low-carbon steel
Corrosion rate
Pitting corrosion
Passivation

ABSTRACT

A grain refined surface layer thicker than 15 μm was fabricated on a low-carbon steel by supersonic fine-particles bombarding (SFPB). The microstructure and electrochemical corrosion properties of the original and the SFPB treated (SFPB-ed) low-carbon steel were characterized by optical microscopy, scanning electron microscopy (SEM), transmission electron microscopy (TEM) and corrosion tests. The results showed that the microstructure of the top surface layer was refined to fine grains with the grain size about 3 μm by SFPB. Dislocation tangles and dense dislocation cells about 500 nm in width were formed in the refined grains. Large amounts of micro-cracks were introduced into the surface layer of the SFPB-ed sample, which led to the increase of its surface roughness. The SFPB treatment accelerated the corrosion of the low-carbon steel in a neutral 3.5 wt.% NaCl solution. The surface layer of the SFPB-ed low-carbon steel was dissolved after a certain time of corrosion, which led to the decrease of its corrosion rate. In a saturated $Ca(OH)_2$ solution with and without Cl^-, the micro-cracks in the surface layer of the SFPB-ed sample did not degrade its passivity properties and pitting resistance, which was due to the superior re-passivation properties of the abundant crystalline defects in its surface layer, such as grain boundaries and dislocations.

1. Introduction

Nanocrystalline (NC) materials have gained increasing scientific attention due to their unique microstructures and properties. Three main types of NC materials, including nano-powder, NC layer and 3-dimensional bulk NC materials have been fabricated [1–7]. In most cases, the failures of materials occur on the surface. Surface engineering may effectively improve the comprehensive property of the material. Surface nanocrystallization techniques have been proved to notably improve the mechanical, physical and chemical properties of various materials [8–13]. Two categories of techniques have been developed to fabricate surface NC materials, namely, surface severe plastic deformation and deposition/sputtering coating methods [4,12–14]. Compared with the coating methods, the surface severe plastic deformation methods can obtain NC surface layers in metals without changing the chemical composition.

Surface severe plastic deformation methods include peening [15–19], mechanical attrition [20–22], rolling [23–25] and supersonic fine-particles bombarding (SFPB) [26–28], among others. These methods have successfully fabricated NC surface layers in various metallic materials, such as irons [21,22], low-carbon steels [16], stainless steels [17,22,26–28] and other metals or alloys [2,11,12,14,19], whose mechanical properties have been significantly improved.

The corrosion resistance of a NC material is an important performance for its industrial application in the future. The influence of grain size of metallic materials on their corrosion resistance has been reported. Studies suggested that grain refinement reduces the corrosion rates of passivity metals and accelerates the corrosion of metals without forming an oxide or passive film [29–31].

Residual stress after mechanical processing is another important factor that has a complex influence on the corrosion resistance.

McMahon et al. [32] investigated the effects of residual stress on corrosion resistance of aluminum alloys and showed that a residual tensile stress promoted corrosion while a residual compressive stress had an opposite effect. Turnbull et al. [33] found that high residual tensile stress induced by grinding caused more severe pitting corrosion of the AISI 304 stainless steel. Denkena et al. [34] reported that the corrosion rate of a Mg–Ca alloy was decreased by a high residual compressive stress derived from deep rolling. Scheel et al. [35] revealed that the corrosion resistance of an Al alloy was significantly improved by inducing a large residual compressive stress near the surface through low plasticity burnishing. Rhouma et al. [36] reported that the pitting corrosion resistance of a 316L stainless steel was improved after inducing a near-surface residual compressive stress.

However, research data found in literature showed opposite results. Op't Hoog et al. [37,38] reported that a large residual stress induced by surface mechanical attrition treatment increased the corrosion rate of

* Corresponding author at: College of Mechanics and Materials, Hohai University, Nanjing 210098, PR China. Tel.: +86 25 8378 7239; fax: +86 25 8378 6046.
E-mail addresses: zhangliuyanjust@163.com (L. Zhang), aibin-ma@hhu.edu.cn (A. Ma), jinghua-jiang@hhu.edu.cn (J. Jiang).

0257-8972/$ – see front matter © 2013 Elsevier B.V. All rights reserved.
http://dx.doi.org/10.1016/j.surfcoat.2013.05.043

Mg alloys. Lü et al. [39] found that surface mechanical attrition treatment improved the corrosion resistance of 316L stainless steel. Li et al. [40] reported that the corrosion rate of Cu in a HNO_3 solution increased with an increase in strain under both tension and compression conditions. Therefore, the effects of residual stress on corrosion resistance are closely related both to material type and to manufacturing process.

Low-carbon steels are widely used in many fields, whose performance could be improved by the surface nanocrystallization treatment. Li et al. [41] reported the effect of grain size on the corrosion resistance of a NC low-carbon steel fabricated through ultrasonic shot peening technique in a 0.05 M H_2SO_4 + 0.05 M Na_2SO_4 solution. When grain size was less than 35 nm, the corrosion rate increased as grain size decreased.

The individual contribution of residual stress, dislocation density and surface properties to corrosion resistance is difficult to be distinguished from the grain refinement process. A specific thermomechanical processing has various effects on electrochemical corrosion behavior of materials in different corrosive mediums. SFPB is a recently developed surface nanocrystallization technique, which has a huge potential in application due to the simple equipment and operations, high efficiency and minimal damage to environment [26–28]. The SFPB technique has barely been used on a low-carbon steel plate.

This paper focuses on the SFPB technique which is used to form NC surface layer on a low-carbon steel plate as well as the effects of the microstructure and surface properties have on its corrosion resistance. This research results will help researchers when applying SFPB.

2. Experimental details

The hot-rolled low-carbon steel plate (wt.%: C, 0.10 to 0.13; Si: 0.11 to 0.15; Mn: 0.38 to 0.45; S: 0.027; P: 0.024 to 0.028; Cr: 0.01; Ni: 0.01; Cu: 0.02; Fe: bal.) with dimensions of 100 mm × 60 mm × 5 mm was used as research material. One side of the plate was first ground with 500-grit SiC paper and subsequently treated by the SFPB machine under 0.18 MPa for 300 s. Stainless balls of 300 μm in diameter were used as particles for bombarding. A supersonic speed short head was used, and the spray angle was 80°. The airflow temperature was 50 °C.

The microstructure of the cross-section perpendicular to the treated surface of the SFPB-ed sample was examined by electron back-scattered diffraction (EBSD). The cross-section was mechanically polished and etched in a weak solution of nitric acid and alcohol. The microstructure of the surface layer of the samples before and after SFPB was characterized by optical microscopy and transmission electron microscopy (TEM, Tecnai G2). Thin foils for TEM observations were prepared by cutting, grinding and twin-jet polishing, and their selected area electron diffraction (SAED) patterns were observed by TEM. The surface morphology of the untreated and SFPB-ed samples was observed by scanning electron microscopy (SEM).

Before corrosion tests, samples with dimensions of 10 mm × 10 mm × 3 mm were cut from the SFPB-ed and untreated plates. Only one surface of each sample was exposed to the electrolyte, with an area of 10 mm^2, while the other surfaces were covered with an epoxy resin. The exposed surface of the SFPB-ed sample was the treated surface.

The corrosion behavior of all the samples was measured by immersion and electrochemical corrosion tests, which were repeated at least three times to ensure reproducibility of the test results.

For the immersion corrosion tests in a 3.5 wt.% NaCl solution, after the set intervals of immersion, the mass loss of the samples was examined by AL204 electronic balance to calculate the corrosion rate (unit: $g \cdot cm^{-2} \cdot h^{-1}$). Corrosion morphologies on the surface of the samples after 72 h and 4000 h of immersion were observed by SEM.

The electrochemical corrosion tests were performed using a Parstat 2273 electrochemical station at 25 °C in a conventional three-electrode cell, with a saturated calomel electrode (SCE) used as reference electrode and a platinum foil as auxiliary electrode. The corrosion mediums included a 3.5 wt.% NaCl solution, a saturated $Ca(OH)_2$ solution and a saturated $Ca(OH)_2$ solution containing 3.5 wt.% NaCl. The potentiodynamic polarization curves of the samples in these mediums were acquired at the same sweep rate of 0.7 $mV \cdot s^{-1}$, and their potential varied from −1 V_{SCE} to −0.3 V_{SCE}, from −1 V_{SCE} to 1 V_{SCE} and from −0.5 V_{SCE} to 0.3 V_{SCE}, respectively. The electrochemical impedance spectroscopy (EIS) studies of the samples in the saturated $Ca(OH)_2$ solution were conducted at the open circuit potential over a frequency range of 10^5 Hz to 10^{-2} Hz, with a single amplitude perturbation of 5 mV.

3. Results and discussion

3.1. Microstructure analysis

The typical microstructure of the low-carbon steel matrix is shown in Fig. 1. The white areas denoted the ferrite grains, and the dark areas indicated pearlite, which were distributed around the

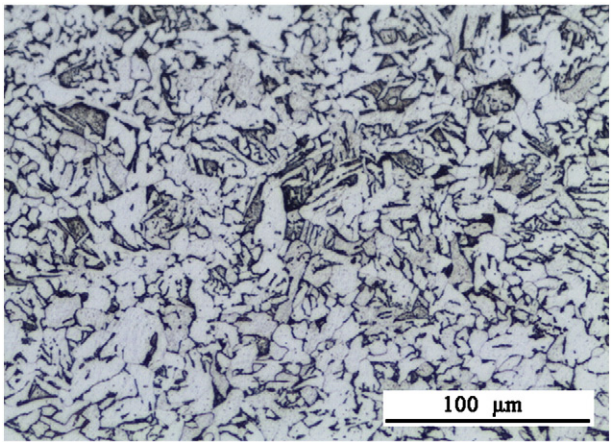

Fig. 1. Microstructure of low-carbon steel matrix.

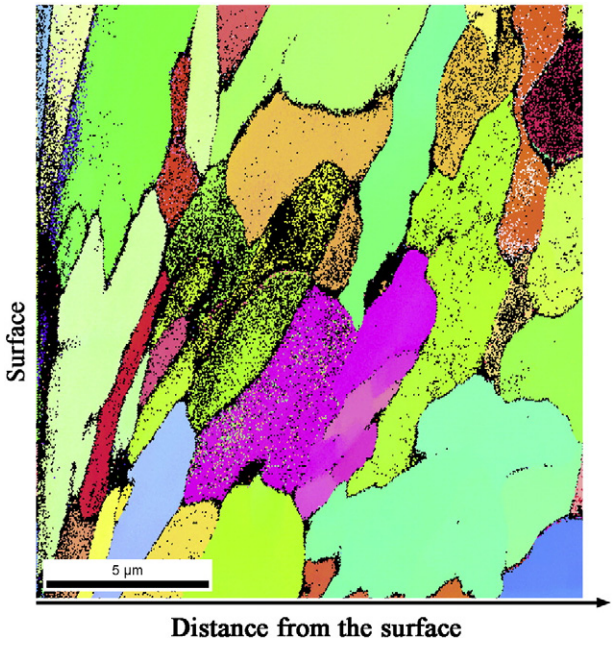

Fig. 2. EBSD image of polished cross-section perpendicular to the SFPB-ed surface of low-carbon steel.